Saudi Pharmaceutical Journal 27 (2019) 341–347

Contents lists available at ScienceDirect

Saudi Pharmaceutical Journal

journal homepage: www.sciencedirect.com

Original article

Mechanistic interaction study of 5,6-Dichloro-2-[2-(pyridin-2-yl)ethyl] isoindoline-1,3-dione with bovine serum albumin by spectroscopic and molecular docking approaches

Mohammed M. Alanazi [a], Abdulrahman A. Almehizia [a], Ahmed H. Bakheit [a,b], Nawaf A. Alsaif [a], Hamad M. Alkahtani [a], Tanveer A. Wani [a,*]

[a] Department of Pharmaceutical Chemistry, College of Pharmacy, King Saud University, P.O. Box 2457, Riyadh 11451, Saudi Arabia
[b] Department of Chemistry, Faculty of Science and Technology, Al-Neelain University, Khartoum, Sudan

ARTICLE INFO

Article history:
Received 29 August 2018
Accepted 5 December 2018
Available online 6 December 2018

Keywords:
BSA
Thermodynamics
Docking
Fluorescence quenching
Spectroscopy

ABSTRACT

A synthesized and promising biologically hypoglycemic compound 5,6-Dichloro-2-[2-(pyridin-2-yl)eth yl]isoindoline-1,3-dione (**5e**) was studied for its binding to a model protein (bovine serum albumin; BSA) by spectroscopic and molecular simulation approaches. Fluorescence studies revealed that **5e** quenched BSA's intrinsic fluorescence by static quenching. The experiments were performed at three different temperatures and the quenching constants and binding constants were evaluated. Stern-Volmer constant (K_{sv}) values decreased from 1.36×10^4 to 1.20×10^4 as the temperature increased suggesting static quenching involvement in the interaction. Decreased binding constants from 1.70×10^4 to 4.57×10^3 at higher temperatures indicated instability of the complex at rising temperatures. Site I (subdomain IIA) of BSA was found to interact with **5e**. The thermodynamic results showed the binding interaction was spontaneous and enthalpy driven. The secondary structure alterations in BSA due to interaction with **5e** were studied by UV–visible, synchronous fluorescence, and three-dimensional fluorescence spectra. The results indicate the **5e** binds effectively to the BSA and thus, this study can be useful in further exploring the pharmacokinetics and pharmacodynamics of **5e**.

1. Introduction

Amongst the biomolecules the proteins are the most important and are involved in numerous biological processes. Protein content in biological fluids is of diagnostic value for determination of several diseased conditions and is also of an immense value in the chemical investigations (Kandagal et al., 2006; Zhu et al., 2007; Suryawanshi et al., 2016). The protein and drug interaction, protein structure and functional changes on biological performance is of great interest to the researchers (Peters, 1996; He and Carter, 1992).

In the transportation and disposition of drugs in biological system serum albumin present in the blood plasma plays a major role. The extensive study of BSA as model protein for these interaction is because of its structural homology to the human serum albumin (Mote et al., 2010; Wang et al., 2007). Structurally BSA consists of three homologous domains and each of these domains consist of two sub-domains namely sub-domain IA, IB, IIA, IIB, IIIA, and IIIB. These sub-domains of BSA are involved in binding the endogenous and/or exogenous ligands. The ligand binding sites of BSA are located in the hydrophobic cavities of sub-domains IIA and IIIA (He and Carter, 1992).

The biological activities of N-substituted phthalimides is well established (Cullen, 2000; Krauss,1998; Rubins, 2000; Rubins and Robins, 2000). The anti-hyperlipidemic and anti-diabetic potential of these compounds have been explored (Kim et al., 2006; Zimmet et al., 2001) The mechanism of hypolipidemic activity of N-substituted phthalimides is supposed to be due to their inhibitory activity against acetyl-CoA (Kim et al., 2006; Betteridge, 1984). The studied compound **5e** (Fig. 1) (Alaa et al., 2011) was found to lower the serum glucose in diabetic rate by 55% and the reduction was

* Corresponding author.
E-mail address: twani@ksu.edu.sa (T.A. Wani).
Peer review under responsibility of King Saud University.

Production and hosting by Elsevier

https://doi.org/10.1016/j.jsps.2018.12.001
1319-0164/

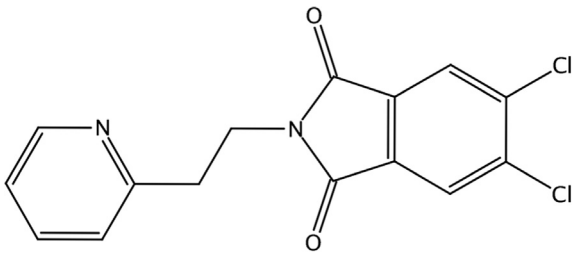

Fig. 1. Chemical structure of 5,6-Dichloro-2-[2-(pyridin-2-yl)ethyl]isoindoline-1,3-dione (**5e**).

more than the standard drug glibenclamide which showed only 51% reduction in the serum glucose levels of diabetic rats. Further, **5e** decreased the cholesterol and triglyceride levels more efficiently than the positive control glibenclamide (Alaa et al., 2011).

Pharmacokinetic and pharmacodynamics of a drug is dependent on the drug-protein interaction. Fluorescence technique are particularly used to explore ligand protein interactions (Chi et al., 2010; Wani et al., 2017a, 2017b, 2017c; Wani et al., 2018a). The affinity of **5e** for BSA was investigated in this study and thus, explore the carrier role of BSA for **5e** under physiological conditions. The binding studies are helpful in understanding the interaction mechanism and designing of suitable ligands. In addition to the fluorescence quenching study, conformational changes in the BSA post interaction were also studied by UV–visible spectroscopy, synchronous fluorescence (SF), and three-dimensional spectroscopy. Different temperatures were used to carry out the binding studies and evaluate the involved thermodynamic processes. Molecular docking studies were also carried out for the ligand and the BSA protein and the obtained results were related to the spectroscopic experimental results.

2. Materials and methods

2.1. Materials

The materials and their procuring sources were as follows: Fatty acid free BSA (Sigma Aldrich; USA); Ibuprofen and phenylbutazone (National Scientific Company; KSA). The **5e** was synthesized (Alaa et al., 2011) in synthetic chemistry laboratory of Pharmaceutical Chemistry Department; College of Pharmacy; King Saud University. The BSA, **5e**, ibuprofen and phenylbutazone stocks were prepared in phosphate buffer (pH 7.4). The water used for buffer preparation was from Elga Purelab (Elga Lab Water UK). Materials of analytical purity were used for the analysis.

2.2. Instrumentation

The fluorescence emission spectra were recorded at three temperatures 298, 305 and 310 K using JASCO spectrofluorometer. A slit width of 5 nm was used for attaining both excitation and emission spectra. An excitation wavelength of 280 nm and emission wavelength of 300–500 nm was used to obtain the fluorescence spectra. The UV–vis absorption spectra were recoded using UV-1800 spectrophotometer from Shimadzu (Japan) The spectra were recorded in the range of 200–500 nm.

2.3. Fluorescence spectral and UV–Vis spectral measurement

The fluorescence spectra of BSA and BSA-**5e** complex were recorded. A fixed concentration of BSA and variable concentrations of **5e** were used to record the spectra. Inner filter effect can lead to reduced fluorescence intensity (FI) and therefore need to be corrected. The inner filter effects were corrected with the equation:

$$F_{cor} = F_{obs} \times e^{(A_{ex}+A_{em})/2} \quad (1)$$

The fluorescence (corrected and observed) were represented by F_{cor} and F_{obs} respectively. The absorption at the excitation and emission wavelength of **5e** were denoted by A_{ex} and A_{em}.

The UV–Vis spectra were recorded at room temperature (298 K) for the BSA and BSA-**5e** complex (fixed BSA concentration and increasing **5e** concentration).

2.4. Synchronous fluorescence (SF)spectral measurement and site binding studies

SF spectra for **5e** and BSA-**5e** complexes were recorded at room temperature (298 K). The scanning intervals $\Delta\lambda$ ($(\Delta\lambda = \lambda_{em} - \lambda_{ex})$ equal to 15 and 60 nm were used to record the spectra. The intervals of $\Delta\lambda$ = 15 nm and 60 nm characterize the tyrosine (Tyr) and tryptophan (Trp) residues respectively. Binding site identification for **5e** on BSA was carried out using displacement studies for site specific markers phenylbutazone and ibuprofen.

2.5. Molecular docking

Molecular simulation experiments were done to study the BSA-**5e**-binding interaction. The interaction was studied using Molecular Operating Environment (MOE) software. Naproxen co-crystallized structure of BSA was acquired from protein data bank; pdb code:4OR0 and the **5e** structure was drawn within MOE (Zhou et al., 2018; Jiang et al., 2018). BSA consists of two homodimer chains, named as A and B. These studies were conducted using the chain B of the BSA homodimer.

3. Results and discussions

3.1. Fluorescence studies

The amino acid residues Trp and Tyr are primarily responsible for a protein's intrinsic fluorescence. It has also been observed that a protein ligand interaction usually reduces the fluorescence intensity of the protein and this reduction is ligand concentration dependent. Thus, the protein ligand interaction can be explored with the help of fluorescence quenching studies. (Chu et al., 2010).

The fluorescence spectra were recorded for BSA whose concentration was held constant and the **5e** concentration was varied. (Fig. 2). A reduction in FI of BSA occurred post interaction with **5e** and got further reduced with increasing **5e** concentration

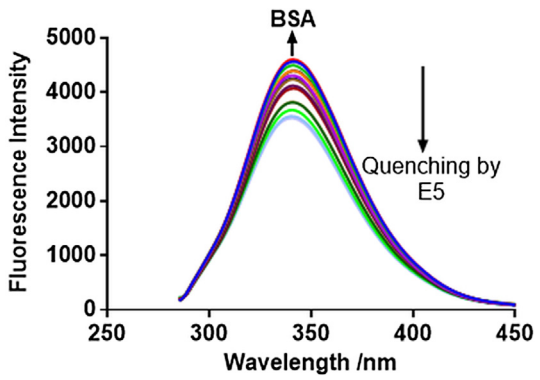

Fig. 2. Fluorescence spectra of BSA (1.5 μM) in the presence of **5e** at 298 K; (**5e** concentration $(1.49 \times 10^{-6}$, 2.99×10^{-6}, 5.98×10^{-6},1.49×10^{-5}, 5.97×10^{-6}, $1.79 \times 10^{-5})$.

suggesting fluorescence quenching. The fluorescence spectra of BSA-**5e** showed a blue shift indicating that the chromophore in the serum albumin shifted towards a more hydrophobic microenvironment. The involved quenching mechanisms could be either static or dynamic quenching or combined dynamic and static quenching (Feitelson, 1964; Wang et al., 2016; Zhang et al., 2017). These two mechanisms are distinguished from one another based on their dependency on temperature and viscosity (Mater, 2010). At high temperatures large diffusion coefficients are observed in dynamic quenching and are further increased with rise in temperature. However, in static quenching as the temperature increases the stability of protein–ligand complex decreases leading to lower quenching constants. However, in case of combined dynamic and static quenching both collision and complex formation occur with the same quencher.

3.2. Quenching mechanism analysis

Stern-Volmer equation was used to elucidate the quenching mechanism between BSA and **5e** (Lakowicz, 2004).

$$\frac{F_0}{F} = 1 + K_{sv}[Q] = 1 + k_q\tau_0[Q] \quad (2)$$

F and F_0 are the FI of BSA in presence and absence of **5e** respectively. K_{sv} represents the Stern -Volmer constant; [Q] Quencher concentration; k_q quenching rate constant; τ_0 excited state lifetime of fluorophore and is valued 10^{-8} S for biomolecules (Lakowicz, 2004; Zhao et al., 2010; Wani et al.,2018b; Hu et al., 2010).

Fig. 3A represents the plot between F_0/F and **5e** at the different temperatures. The plots exhibited a good linear relationship and the results are given in Table 1. The K_{sv} values decreased at higher temperatures indicating formation of a ground state complex between BSA and **5e**. Formation of complex between BSA and **5e** infers involvement of static quenching. The maximum achievable value for the dynamic quenching constant for biopolymers is $2 \times 10^{10}\,LM^{-1}\,S^{-1}$ (Ware, 1962). The quenching constant values attained were greater than $2 \times 10^{10}\,LM^{-1}\,S^{-1}$ as given in Table 1, further indicates the formation of complex and involvement of static quenching between BSA and **5e**.

Table 1
K_{SV} and K_q values for the binding interaction of **5e** and BSA at different temperatures.

T(K)	R	$K_{sv} \pm SD \times 10^4$ (L mol^{-1})	$k_q \times 10^{12}$ (L mol^{-1} s^{-1})
298	0.9958	1.36 ± 0.025	1.36
305	0.9993	1.26 ± 0.016	1.26
310	0.9973	1.20 ± 0.020	1.20

3.3. Binding constant and binding site

Therapeutic potential of drugs depends on the in-vivo binding potential of these drugs and this ability can influence their stability and toxicity in a therapeutic process. The binding interaction evaluation between BSA and **5e** was based on the binding constants calculated from FI data obtained at different temperatures. The free and bound molecular equilibrium is given by the double log regression curve (Zhao et al., 2009; Rabbani et al., 2017a, 2017b. The following equation represents this equilibrium:

$$\log\frac{(F_0 - F)}{F} = \log K_b + n\log[Q] \quad (3)$$

In the plot log $[(F_0 - F)/F]$ Vs log [Q] (Fig. 3B), slope 'n' represents stoichiometry of binding and the binding constant K_b is calculated from the intercept (Table 2). Single binding site for **5e** present on BSA molecule is inferred from the fact that n is approximately equal to unity. This binding strength determines the ability of the drug to diffuse from the bound protein to its target of action (Rabbani et al., 2014; Colmenarejo et al.,2001). The ligands bind to the protein mostly in a reversible fashion and exhibit the binding affinities ranging from $(1–15) \times 10^4\,L\,M^{-1}$ (Dufour and Dangles, 2005). The K_b values obtained showed a decrease at higher temperatures indicating instability of BSA-**5e** complex. Also, the complex formed may be reversible since the binding between BSA and **5e** is moderate.

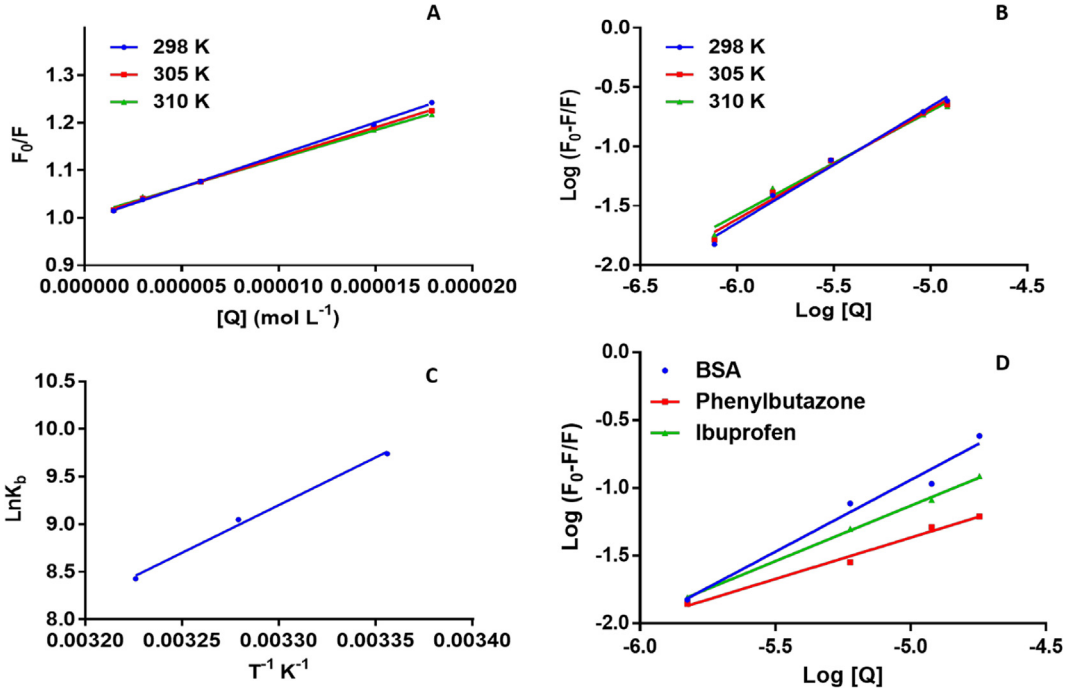

Fig. 3. The plots for interaction between BSA with **5e** at different temperatures [A]: Stern–Volmer Plot, [B]: Binding Constant log $[(F_0 - F)/F]$ Vs log[Q], [C]: Van't Hoff Plot, [D]: Binding constant in presence of site markers at 298 K.

Table 2
Binding and thermodynamic parameter values for the binding interaction of **5e** and BSA at different temperatures.

T(K)	R	Log K_b ± SD	K_b (L mol^{-1})	n	ΔG (kJ mol^{-1})	ΔH (kJ mol^{-1})	ΔS (J mol^{-1} K^{-1})
298	0.9887	4.23 ± 0.013	1.70×10^4	0.98	−26.48	−172	−485
305	0.9874	3.94 ± 0.016	8.71×10^3	0.92	−24.54		
310	0.9895	3.66 ± 0.010	4.57×10^3	0.87	−22.11		

3.4. Binding site identification

The binding site identification of **5e** on BSA was carried out by site competition of **5e** with site specific markers phenylbutazone and ibuprofen (Rabbani et al., 2018). Phenylbutazone is specific marker for site I whereas, ibuprofen is specific marker for site II of BSA. A reduction in FI of BSA was observed on addition of phenylbutazone and ibuprofen. However, phenylbutazone caused a higher decrease in the fluorescence intensity compared to ibuprofen. The calculated binding constants for BSA-**5e**, BSA-phenylbutazone-**5e**, and BSA-ibuprofen-**5e** were 1.62×10^4, 0.48×10^2 and 0.91×10^3 respectively (Fig. 3D). Lower binding constants were observed for the phenylbutazone and ibuprofen complexes in comparison to the BSA-**5e**. Site I (phenylbutazone) Sub-domain IIA as the binding site for **5e** was concluded from the fact that the decrease in the binding constant was much more than that observed for ibuprofen.

3.5. Synchronous fluorescence (SF) and Three-dimensional (3D) studies

The SF spectroscopy is mostly utilized to characterize and understand the effect of interaction between the protein and ligand. The SF spectroscopy gives information about microenvironment of chromophores present in the protein. The two amino acid residues mainly involved in the fluorescence of proteins are Trp, Tyr, and Phe. The difference Δλ ($\Delta\lambda = \lambda_{em} - \lambda_{ex}$) (Lakowicz, 2004) reflects the spectral characteristics and nature of chromophores. The effect of varied concentrations of **5e** addition on the fluorescence quenching of Tyr and Trp residues of BSA at Δλ = 15 and 60 nm respectively was studied. No change was observed in the emission wavelengths at either Δλ = 15 or 60 nm (Fig. 4). Therefore, it is suggested that the amino acid residues Trp and Tyr polarity present in BSA was slightly altered by **5e**.

The 3D fluorescence spectroscopy provides information regarding the configurational changes that might have occurred in the protein after interacting with the ligands (Loyd and Evett, 1977). The 3D data is presented in the (Fig. 5) and the two peaks found were Peak I and Peak II. The Peak I and II were observed at the excitation wavelength of 230 and 280 nm respectively. Peak I is attributed to the pi-pi transition of polypeptides (Rayleigh scattering peak) whereas, Peak II is attributed to the fluorescent amino acid residues present in BSA. Peak II is attributed to the intrinsic fluorescence of tryptophan and tyrosine residues. These amino acid residues are linked to the conformational changes in the peptide backbone that is associated with helix-transformation. Since there was considerable reduction in BSA fluorescence intensity post **5e** addition, it was concluded that peptide backbone (tryptophan and tyrosine) was altered. Thus, conformational changes are suggested to have occurred in BSA indicating complex formation between the BSA and **5e**.

3.6. Thermodynamic studies

The interaction forces that might occur between the proteins and ligands are established with the help of thermodynamic studies. The type of the interaction between protein and the ligand are characterized by their signs and the magnitude of thermodynamic parameters. The following thermodynamic parameters (ΔG°) Gibbs free energy; (ΔH°) change of enthalpy and (ΔS°) change of entropy were explored to identify the interaction forces between **5e** and BSA (Ross and Subramanian, 1981). Value of $\Delta H^{\circ} > 0$ and $\Delta S^{\circ} > 0$, indicate hydrophobic interaction forces whereas, $\Delta H^{\circ 0} < 0$ and $\Delta S^{\circ 0} < 0$ indicate van der Waals forces and hydrogen-bonding. Electrostatic forces are said to be involved in the interaction in case $\Delta H^{\circ} < 0$ and $\Delta S^{\circ} > 0$.

Van't Hoff equation was used to calculate the thermodynamic interaction parameters:

$$\ln K_b = -\frac{\Delta H^{\circ}}{RT} + \frac{\Delta S^{\circ}}{R} \quad (4)$$

where K_b is the binding constant, R is the universal gas constant, T is temperature in kelvins. The slope of the van't Hoff equation gives us the enthalpy change ΔH°. The free energy change is given with the equation:

$$\Delta G^{\circ} = \Delta H^{\circ} - T\Delta S^{\circ} = -RT\ln K_b \quad (5)$$

The thermodynamic parameters were calculated from the van't Hoff plot (Fig. 3C). The thermodynamic results in Table 2 indicate that the interaction between BSA and **5e** was spontaneous in nature since, ΔG° attained a negative value. Since both ΔH° and ΔS° were negative and therefore, suggested an enthalpy driven interaction between BSA and **5e**.

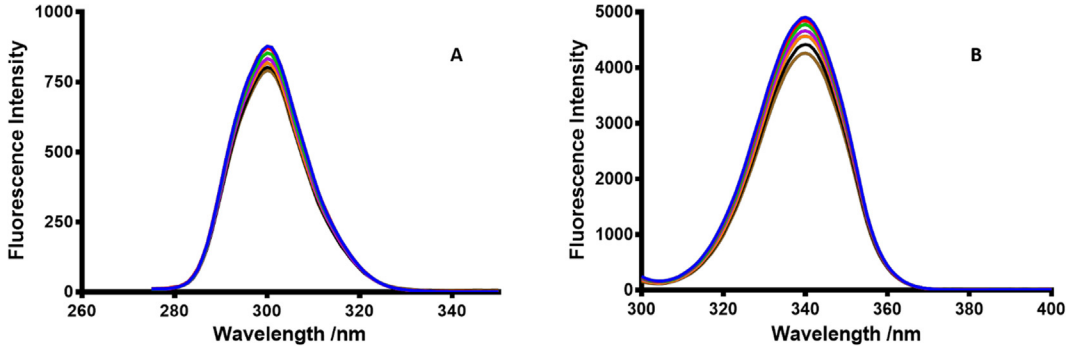

Fig. 4. Synchronous fluorescence of BSA-**5e** complex at 298 K [A] Δλ = 15 nm and [B] Δλ = 60 nm.

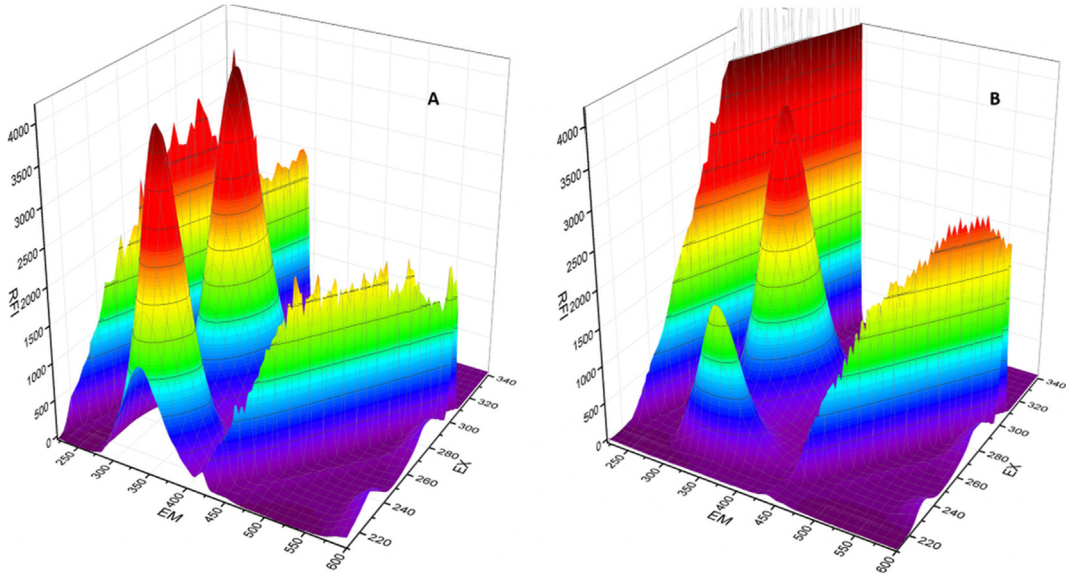

Fig. 5. Three-dimensional fluorescence analysis, BSA [A]: BSA-**5e** Complex [B].

3.7. UV–vis absorption studies

The UV–vis absorption methodology was used to study the possible BSA structural alterations and BSA and **5e** complex (Shi et al., 2018a, 2018b). Spectra for UV-absorption of BSA (1.5 μM) alone and in presence of **5e** at room temperature were recorded (Fig. 6). The following **5e** concentrations used were (1.49×10^{-6}, 2.99×10^{-6}, 5.98×10^{-6}, 1.49×10^{-5} and 1.79×10^{-5}) for the analysis. The UV-absorption spectra display in the range influence of **5e** on the absorption spectrum of BSA. The spectrum showed

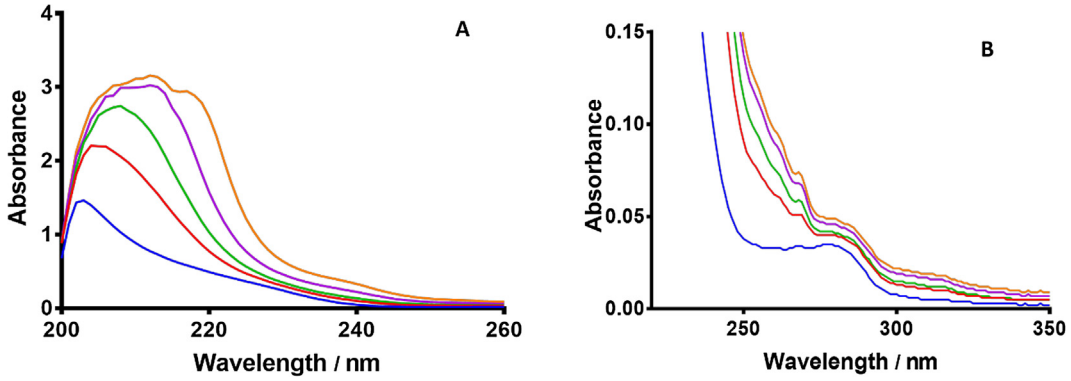

Fig. 6. UV-absorption spectra of BSA and BSA-**5e** complex.

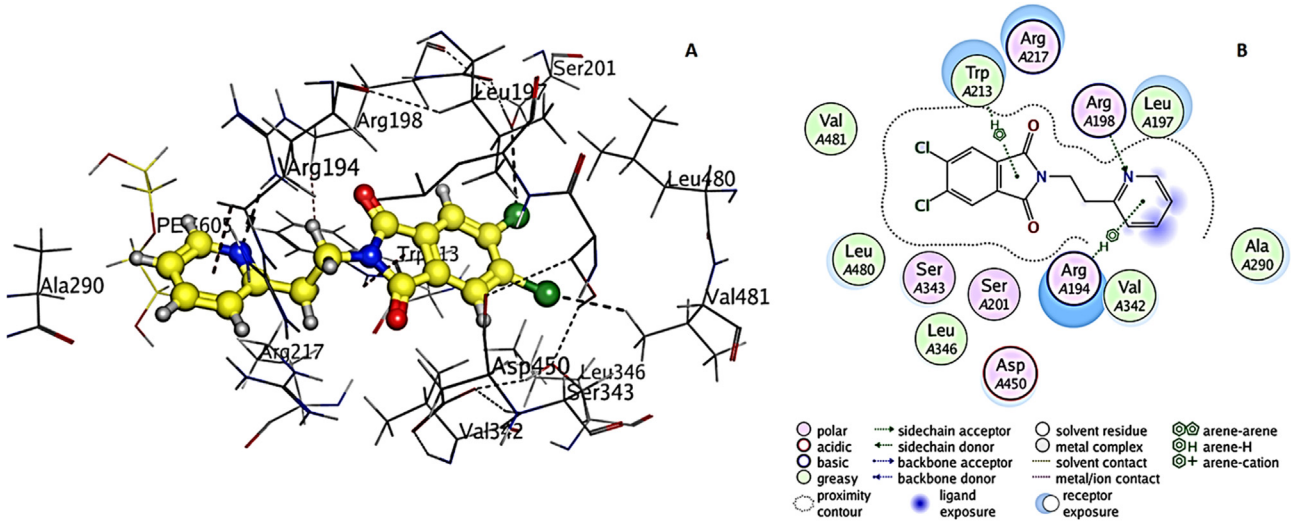

Fig. 7. [A] Three dimensional representation of the interaction of **5e** with BSA. [B] A two dimensional representation of amino acids that surround **5e**.

two bands of absorption for BSA and the stronger band occurred at 210 and whereas the weak band occurred at near 280 nm. The 210 nm band characterize conformational structure of the BSA whereas, the 280 nm band characterizes the $\pi \rightarrow \pi$ transition because of aromatic amino acids. An increased absorption intensity was detected at both the band points as the concentration of **5e** was increased suggesting formation of complex between BSA and **5e**. Further, a redshift was seen at near 210 nm in the absorption spectrum which also indicated complex formation.

3.8. Molecular modeling study

The docking was carried out to further ascertain the BSA binding site to bind **5e** (Fig. 7). The binding energy of **5e** at subdomain IIA was -26.63 kJ mol^{-1}, and was lower than the binding energy of **5e** on sub-domain IIIA (-25.31 kJ mol^{-1}). This indicated the preferred binding site for **5e** to be site I of subdomain IIA and the similar results were seen in binding site identification studies. Also, **5e** was observed to be inside the hydrophobic cavity of site I; Fig. 7A.

These results clearly help in understanding the fluorescence quenching behavior of BSA emission in presence of **5e** (Shi et al., 2018a, 2018b). The docking results are also in agreement with the thermodynamic studies as hydrogen bonds were seen between the Arg-198 and **5e** whereas, Pi-H bonds were observed between Arg-194 and Trp-213 residues of BSA (Fig. 7B). The docking results also showed that **5e** interacted with hydrophobic amino acids (Ala-209, Val-481, Val-342, Leu-480, Leu-346, Leu-197. Polar amino acid residues (Trp-213, Ser-201, Ser-343) and charged residues (Arg-217, Arg-198, Arg-194, Asp-450) also interacted with **5e**. The free binding energy (-26.63 kJ mol^{-1}) from the docking procedures was close to the free binding energy value obtained experimentally (Table 2).

4. Conclusion

Different spectroscopic methods were used for the detailed study of interaction hypoglycemic compound **5e** with BSA. Experimental and docking approaches were used to explore this interaction. BSA and **5e** formed a complex and static fluorescence quenching mechanism is suggested to be involved in the interaction. The negative Gibbs free energy suggested a spontaneous interaction between BSA and **5e**. The thermodynamic results also suggested involvement of hydrogen-bonding in the interaction. Conformational changes were also suggested in the BSA after interaction with **5e**. All these results indicate that **5e** can bind to serum albumin, thus, this study can be of helpful in further pharmacokinetic development of **5e**.

Conflict of interest

There is no conflict of interest over the contents of this article.

Acknowledgments

The authors extend their sincere appreciation to the Deanship of Scientific Research and the Research Center, College of Pharmacy, King Saud University for funding the research project.

References

Alaa, A.-M., El-Azab, A.S., Attia, S.M., Al-Obaid, A.M., Al-Omar, M.A., El-Subbagh, H.I., 2011. Synthesis and biological evaluation of some novel cyclic-imides as hypoglycaemic, anti-hyperlipidemic agents. Eur. J. Med. Chem. 46, 4324–4329.
Betteridge, J., 1984. Diabetes lipids and atherosclerosis. Pract. Diabetes Int. 1, 26–30.
Chi, Z., Liu, R., Teng, Y., Fang, X., Gao, C., 2010. Binding of oxytetracycline to bovine serum albumin: spectroscopic and molecular modeling investigations. J. Agric. Food Chem. 58, 10262–10269.
Colmenarejo, G., Alvarez-Pedraglio, A., Lavandera, J.L., 2001. Cheminformatic models to predict binding affinities to human serum albumin. J. Med. Chem. 44, 4370–4378.
Cullen, P., 2000. Evidence that triglycerides are an independent coronary heart disease risk factor. Am. J. Cardiol. 86, 943–949.
Dufour, C., Dangles, O., 2005. Flavonoid–serum albumin complexation: determination of binding constants and binding sites by fluorescence spectroscopy. Biochim. Biophys. Acta 1721, 164–173.
Feitelson, J., 1964. On the mechanism of fluorescence quenching. Tyrosine and similar compounds. J Phys Chem 68, 391–397.
He, X.M., Carter, D.C., 1992. Atomic structure and chemistry of human serum albumin. Nature 358, 209.
Hu, Y.-J., Ou-Yang, Y., Dai, C.-M., Liu, Y., Xiao, X.-H., 2010. Binding of berberine to bovine serum albumin: spectroscopic approach. Mol. Biol. Rep. 37, 3827–3832.
Jiang, T.Y., Zhou, K.L., Lou, Y.Y., Pan, D.Q., Shi, J.H., 2018. Probing the behavior of bovine serum albumin upon binding to atenolol: insights from spectroscopic and molecular docking approaches. J. Biomol. Struct. Dyn. 36, 1095–1107.
Kandagal, P., Ashoka, S., Seetharamappa, J., Shaikh, S., Jadegoud, Y., Ijare, O., 2006. Study of the interaction of an anticancer drug with human and bovine serum albumin: spectroscopic approach. J. Pharm. Biomed. Anal. 41, 393–399.
Kim, S.H., Hyun, S.H., Choung, S.Y., 2006. Anti-diabetic effect of cinnamon extract on blood glucose in db/db mice. J. Ethnopharmacol. 104, 119–123.
Krauss, R.M., 1998. Atherogenicity of triglyceride-rich lipoproteins. Am. J. Cardiol. 81, 13B–17B.
Lakowicz, J.R., 2004. Principles of Fluorescence Spectroscopy, (1999). Kluwer Academic/Plenum Publishers, New York.
Loyd, J.B., Evett, I.W., 1977. Prediction of peak wavelengths and intensities in synchronously excited fluorescence emission spectra. Anal. Chem. 49, 1710–1715.
Mater, J.H., 2010. 175, 985–991.
Mote, U., Bhattar, S., Patil, S., Kolekar, G., 2010. Interaction between felodipine and bovine serum albumin: fluorescence quenching study. Luminescence 25, 1.
Peters, T., 1996. Metabolism: albumin in the body. All About Albumin Biochemistry, Genetics, And Medical Applications.
Rabbani, G., Baig, M.H., Jan, A.T., Lee, E.J., Khan, M.V., Zaman, M., Farouk, A.E., Khan, R.H., Choi, I., 2017a. Binding of erucic acid with human serum albumin using a spectroscopic and molecular docking study. Int. J. Biol. Macromol. 105, 1572–1580.
Rabbani, G., Khan, M.J., Ahmad, A., Maskat, M.Y., Khan, R.H., 2014. Effect of copper oxide nanoparticles on the conformation and activity of β-galactosidase. Colloids Surf. B Biointerf. 123, 96–105.
Rabbani, G., Baig, M.H., Lee, E.J., Cho, W.K., Ma, J.Y., Choi, I., 2017b. Biophysical study on the interaction between eperisone hydrochloride and human serum albumin using spectroscopic, calorimetric, and molecular docking analyses. Mol. Pharm. 14, 1656–1665.
Rabbani, G., Lee, E.J., Ahmad, K., Baig, M.H., Choi, I., 2018. Binding of tolperisone hydrochloride with human serum albumin: effects on the conformation, thermodynamics, and activity of HSA. Mol. Pharm. 15, 1445–1456.
Ross, P.D., Subramanian, S., 1981. Thermodynamics of protein association reactions: forces contributing to stability. Biochemistry 20, 3096–3102.
Rubins, H.B., Robins, S.J., 2000. Conclusions from the VA-HIT study. Am. J. Cardiol. 86, 543–544.
Rubins, H.B., 2000. Triglycerides and coronary heart disease: implications of recent clinical trials. J. Cardiovasc. Risk 7, 339–345.
Shi, J.H., Zhou, K.L., Lou, Y.Y., Pan, D.Q., 2018a. Multi-spectroscopic and molecular modeling approaches to elucidate the binding interaction between bovine serum albumin and darunavir, a HIV protease inhibitor. Spectrochim. Acta A Mol. Biomol. Spectrosc. 188, 362–371.
Shi, J.H., Lou, Y.Y., Zhou, K.L., Pan, D.Q., 2018b. Elucidation of intermolecular interaction of bovine serum albumin with Fenhexamid: a biophysical prospect. J. Photochem. Photobiol. B 1 (180), 125–133.
Suryawanshi, V.D., Walekar, L.S., Gore, A.H., Anbhule, P.V., Kolekar, G.B., 2016. Spectroscopic analysis on the binding interaction of biologically active pyrimidine derivative with bovine serum albumin. J. Pharm. Anal. 6, 56–63.
Wang, Q., Huang, C.R., Jiang, M., Zhu, Y.Y., Wang, J., Chen, J., Shi, J.H., 2016. Binding interaction of atorvastatin with bovine serum albumin: spectroscopic methods and molecular docking. Spectrochim. Acta A Mol. Biomol. Spectrosc. 156, 155–163.
Wang, Y.-Q., Zhang, H.-M., Zhang, G.-C., Tao, W.-H., Fei, Z.-H., Liu, Z.-T., 2007. Spectroscopic studies on the interaction between silicotungstic acid and bovine serum albumin. J. Pharm. Biomed. Anal. 43, 1869–1875.
Wani, T.A., AlRabiah, H., Bakheit, A.H., Kalam, M.A., Zargar, S., 2017a. Study of binding interaction of rivaroxaban with bovine serum albumin using multi-spectroscopic and molecular docking approach. Chem. Cent. J. 11, 134.
Wani, T.A., Bakheit, A.H., Abounassif, M., Zargar, S., 2018a. Study of interactions of an anticancer drug neratinib with bovine serum albumin: spectroscopic and molecular docking approach. Front. Chem. 6, 47.
Wani, T.A., Bakheit, A.H., Al-Majed, A.-R.A., Bhat, M.A., Zargar, S., 2017b. Study of the Interactions of Bovine Serum Albumin with the New Anti-Inflammatory Agent 4-(1, 3-Dioxo-1, 3-dihydro-2H-isoindol-2-yl)-N′-[(4-ethoxy-phenyl) methylidene] benzohydrazide using a multi-spectroscopic approach and molecular docking. Molecules 22, 1258.

Wani, T.A., Bakheit, A.H., Ansari, M.N., Al-Majed, A.R.A., Al-Qahtani, B.M., Zargar, S., 2018b. Spectroscopic and molecular modeling studies of binding interaction between bovine serum albumin and roflumilast. Drug Des., Dev. Therapy 12, 2627–2634.

Wani, T.A., Bakheit, A.H., Zargar, S., Hamidaddin, M.A., Darwish, I.A., 2017c. Spectrophotometric and molecular modelling studies on in vitro interaction of tyrosine kinase inhibitor linifanib with bovine serum albumin. PloS One 12. e0176015.Z.

Ware, W.R., 1962. Oxygen quenching of fluorescence in solution: an experimental study of the diffusion process. J. Phys. Chem. 66, 455–458.

Zhao, L., Liu, R., Zhao, X., Yang, B., Gao, C., Hao, X., Wu, Y., 2009. New strategy for the evaluation of CdTe quantum dot toxicity targeted to bovine serum albumin. Sci. Total Environ. 407, 5019–5023.

Zhang, Y.F., Zhou, K.L., Lou, Y.Y., Pan, D.Q., Shi, J.H., 2017. Investigation of the binding interaction between estazolam and bovine serum albumin: multi-spectroscopic methods and molecular docking technique. J. Biomol. Struct. Dyn. 35 (16), 3605–3614.

Zhao, X., Liu, R., Chi, Z., Teng, Y., Qin, P., 2010. New insights into the behavior of bovine serum albumin adsorbed onto carbon nanotubes: comprehensive spectroscopic studies. J. Phys. Chem. B 114, 5625–5631.

Zhou, K.L., Pan, D.Q., Lou, Y.Y., Shi, J.H., 2018. Intermolecular interaction of fosinopril with bovine serum albumin (BSA): the multi-spectroscopic and computational investigation. J. Mol. Recognit. (16) e2716

Zhu, X., Sun, J., Hu, Y., 2007. Determination of protein by hydroxypropyl-β-cyclodextrin sensitized fluorescence quenching method with erythrosine sodium as a fluorescence probe. Anal Chim. Acta 596, 298–302.

Zimmet, P., Alberti, K., Shaw, J., 2001. Global and societal implications of the diabetes epidemic. Nature 414, 782.